

# Ensemble density functional theory for inhomogeneous fractional quantum Hall systems

O. Heinonen, M. J. Lubin, and M. D. Johnson

Department of Physics, University of Central Florida,  
Orlando, FL 32816-2385

## Introduction

The fractional quantum Hall effect (FQHE) occurs in a two-dimensional electron gas (2DEG) in a strong magnetic field oriented perpendicular to the plane of the electrons[1]. The effect was discovered as a transport anomaly. In a transport measurement it is noted that at certain strengths  $B_c(n)$ , which depend on the density  $n$  of the 2DEG, current can flow without any dissipation. That is, there is no voltage drop along the flow of the current. At the same time, the Hall voltage perpendicular to both the direction of the current and of the magnetic field is observed to attain a quantized value for a small, but finite, range of magnetic field or density, depending on which quantity is varied in the experiment. The effect is understood to be the result of an excitation gap in the spectrum of an infinite 2DEG at these magnetic fields. A convenient measure of the density of a 2DEG in a strong magnetic field is given by the filling factor  $\nu = 2\pi \hbar^2 n / eB$ , with  $\lambda_B = \hbar c / (eB)$  the magnetic length. The filling factor gives the ratio of the number of particles to the number of available states in a magnetic sub-band (Landau level), or, equivalently, the number of particles per flux quantum  $\phi_0 = \hbar c / e$ . The quantum Hall effect was first discovered[2] at integer filling factors. In this integer quantum Hall effect, the energy gap is nothing but the kinetic energy gap  $\hbar^2 \omega_c = \hbar eB / (m^* c)$ . Later, the fractional quantum Hall effect (FQHE) was discovered[3] at certain rational filling factors of the form  $\nu = p/q$ , with  $p$  and  $q$  relative primes, and  $q$  odd. In the FQHE, the excitation gap is a consequence of the strong electron-electron correlations. Therefore, any computational approach to the quantum Hall effect must accurately treat the electron correlations in order to capture the FQHE at all. We emphasize that this fact makes any density functional approach to the FQHE qualitatively different from 'standard' applications to atomic, molecular or condensed matter systems. In such standard applications, the electron correlations usually give a quantitatively important correction of the order of perhaps 10-20% but do not usually qualitatively change the results in a fundamental way. Furthermore, standard applications of density functional theory do not require ensemble density functional theory (in such applications, the systems under considerations are typically pure-state v-representable). Our work represents (to the best of our knowledge) the first practical

applications of ensemble density functional theory to a system which is not pure-state v-representable.

Our understanding of the origin of the FQHE started with Laughlin's seminal paper of 1983 [4], which dealt with the simplest fractions  $\nu = 1/m$ , with  $m$  an odd integer. At these values of  $\nu$ , there are on the average  $m$  magnetic flux quanta  $\phi_0 = hc/e$  per electron. Laughlin constructed a variational wavefunction for spin-polarized systems in strong magnetic fields, strong enough that the splitting  $\hbar\omega_c$  between the magnetic subbands, or Landau levels, can be taken to be infinite. The wavefunction can then be constructed from single-particle states entirely within the lowest Landau level. Laughlin wrote the variational wavefunction as

$$\psi_m = \frac{1}{N!} \prod_{i,j} (z_i - z_j)^m \exp \left( -\frac{1}{4} \sum_k |z_k|^2 \right) \quad (1)$$

where  $z_j = x_j + iy_j$  is the coordinate of the  $j$ th electron in complex notation. This wavefunction is an eigenstate of angular momentum. Laughlin demonstrated that the system having the wavefunction Eq. (1) is an incompressible liquid with  $\nu = 1/m$ ,  $m$  odd, with an energy gap to excitations, and that the elementary excitations are fractionally charged quasiholes or quasi-particles of charge  $e^* = e/m$ . The origin of the energy gap can be understood in the so-called pseudo-potential representation of the electron-electron interactions [5]. Here, the electron-electron interaction  $V(r_i - r_j)$  between electrons  $i$  and  $j$  is decomposed into strengths  $V_\ell$  in relative angular momentum channels  $\ell = 0; 1; 2; \dots$ , of the two electrons. For any realistic interaction  $V(r_i - r_j)$ , it turns out that  $V_0 > V_1 > V_2 > \dots$ . Consider the case  $\nu = 1/3$ . In this case, the lowest angular momentum pseudo-potential that enters into the  $m = 3$  Laughlin description is  $V_1$ , the interaction energy of two electrons of unit relative angular momentum (in units of  $\hbar$ ). (Only odd relative angular momenta are permissible for spin-polarized electron wavefunctions, since they have to be anti-symmetric under interchange of electron coordinates.) The Laughlin wavefunction is a very cleverly constructed highly correlated state which completely excludes unit relative angular momentum between any two electrons, and is furthermore the only state which satisfies this property at  $\nu = 1/3$ . Therefore, any excited state at this filling factor must contain some electrons with unit relative angular momentum. The energy gap is due to the cost of this, and hence is of order  $V_1$ . Figure 1 depicts the exchange-correlation energy per particle for infinite, homogeneous FQHE systems vs. filling factor. The cusps at filling factors  $\nu = 1/3; 2/5; 3/5; 2/3; 4/3$ , and  $\nu = 7/5$  have been included to scale. Note that these cusps are barely visible on this scale, yet they are responsible for all the physics of the FQHE!

Finite systems, and spins

We have outlined above how the electron-electron interactions in an infinite, homogeneous system produce the excitation gap. It is important to note that these gaps are only for excitations in the bulk of the system. When a system is bounded there must be gapless excitations located at the boundaries of the system [6, 7]. Since all experimental systems are finite and inhomogeneous, the low-energy properties probed by experiments are necessarily determined by the gapless edge excitations. Advances in semiconductor nanofabrication technologies have led to the possibility of manufacturing systems which are extremely inhomogeneous, and in practice dominated by edges. As an example, recent experiments have even been performed on tiny quantum dots, containing about 30 electrons [8, 9]. Also, edge structures in inhomogeneous systems

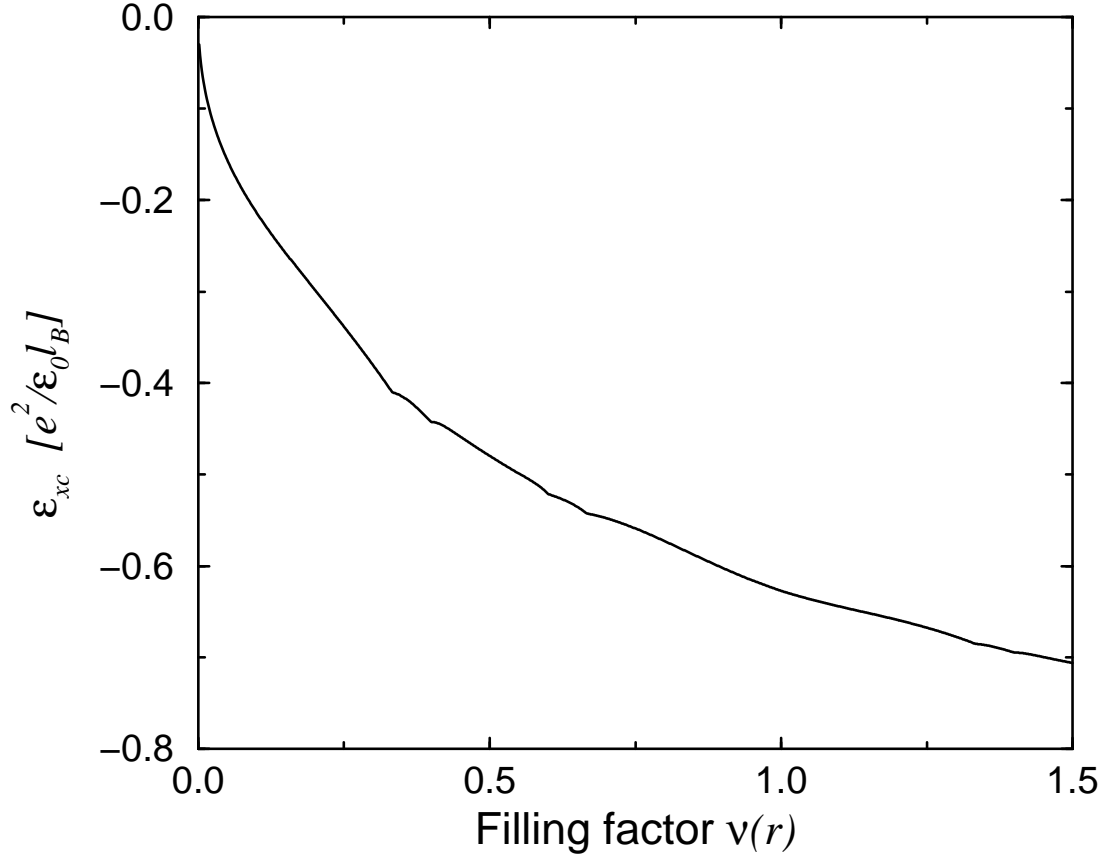


Figure 1. The ground state energy  $\epsilon_{xc}$  per particle of an infinite, homogeneous, spin-polarized FQHE system is depicted as a function of filling factor. The cusps at  $\nu = 1/3; 2/5; 3/5; 2/3; 4/3$ , and  $\nu = 7/5$  are included. In this plot, the smooth part of the exchange-correlation energy was obtained from the Levesque-Weiss-MacDonald interpolation formula Eq. (7)

have been studied directly using capacitance spectroscopy [10], time-resolved measurements of edge magnetoplasmons (the gapless modes along the boundary) [11], and by surface acoustic wave techniques capable of resolving very small inhomogeneities in the electron density [12].

So far, we have limited the discussion to spin-polarized system. At first look it seems reasonable that in the strong magnetic fields used in experiments on QHE systems the Zeeman splitting  $g_B B$ , where  $g$  is the effective Lande factor and  $B$  the Bohr magneton, is large enough that the high-energy spin direction is energetically inaccessible. However, two factors conspire to make the Zeeman splitting very low in GaAs systems. First of all, spin-orbit coupling in the GaAs conduction band effectively lowers the Lande factor to  $g \approx 0.44$ . Second, the low effective mass,  $m \approx 0.067m_e$ , further reduces the ratio of Zeeman energy to cyclotron energy to about 0.02, compared to its value of unity for free electrons. For magnetic fields of about  $1 \times 10$  T, the Coulomb energy scale of the electron-electron interactions,  $e^2/(\epsilon_0 l_B)$ , where  $\epsilon_0 \approx 12.4$  is the static dielectric constant, is of the same order as the cyclotron energy. As a first approximation, one should then set the Zeeman energy to zero, rather than infinite, since it is two orders of magnitude smaller than the other energy scales. As a consequence, the spin-degree of freedom is governed by the electron-electron interactions, rather than by the Zeeman energy. This dramatically changes the nature of the low-energy

bulk single-particle excitations near filling factors of the form  $\nu = 1/m$ , with  $m$  odd, from single-particle spin-orbits to charge-spin textures. In these objects, loosely called skyrmions, the spin density varies smoothly over a distance of several magnetic lengths, so that the system can locally take advantage of the exchange energy. Skyrmions in the quantum Hall effect were first predicted by Sondhi et al. [13]. Recent experiments [14] measuring the spin-polarization near  $\nu = 1$  have provided evidence for this. According to calculations by Karlhede et al. [15], the skyrmion excitations in an inhomogeneous system may lead to charge-spin textures appearing at the edges of QHE systems, which would dramatically change our understanding of QHE edges.

In order to accurately understand the experiments and inhomogeneous FQHE systems in general, we must have a way of accurately calculating their properties, including the spin degrees of freedom. Certain aspects of inhomogeneous FQHE systems have been studied by different techniques. For example, field theories can be constructed to study the low-energy limit of the gapless edge excitations for spin-polarized systems [16], or the spin texture on the edge of an inhomogeneous Hall bar [15]. However, effective field theories typically do not give accurate quantitative results, other than for e.g. critical exponents near fixed points. So-called composite fermion methods have been used for non-interacting composite fermions [17] and in a Hartree approximation to study finite spin-polarized FQHE systems [18, 19, 20]. In this approach, the Chern-Simons term, arising from the singular gauge transformation, is replaced by its smooth spatial average, and the composite fermion mass, which is not well known, has to be put in by hand. The electron-electron interaction can then be treated in a self-consistent Hartree approximation. The hope is then that the most important aspects of the electron-electron correlations are included in this approximation. Near  $\nu = 1$ , at which the Slater determinant  $\Psi_1$  is the exact ground state, it makes sense to use the Hartree-Fock approximation, and the stability of a spin-polarized quantum dot at  $\nu = 1$  as a function of confining potential has been studied in this approximation [21, 22]. The edge structure of spin-polarized systems has also been studied using semiclassical methods [23, 24], in which the electron-electron interaction is included at the Hartree level and it is furthermore assumed that all potentials vary on a length scale much larger than  $\ell_B$ . Beenakker [23], and Chklovskii, Shklovskii and Glazman [24] demonstrated that the edge of an integer quantum Hall system, in which the correlation energies between the electrons can be ignored, consists of a sequence of compressible and incompressible strips. The widths of the incompressible strips is determined by the length over which the effective confining potential (external plus Hartree) varies an amount equal to the energy gap  $\hbar\omega_c$ . The origin of the compressible and incompressible strips are the energy gaps, which are the kinetic energy gaps  $\hbar\omega_c$  in the case of the integer quantum Hall effect. But it is easy to generalize the argument to include the energy gaps causing the FQHE [24]. The conclusion is then that there should be compressible and incompressible strips, with the density of each incompressible strip fixed at the value of an FQHE fraction. The width of each incompressible strip is then fixed by the length over which the effective confining potential varies an amount equal to the energy gap of the FQHE fraction corresponding to the density of that strip.

Quantum dots including the spin degree of freedom have also been studied by direct numerical diagonalizations [25]. These calculations demonstrated the importance of the spin degree of freedom. At the present, numerical diagonalizations are limited to systems with of the order of 10 electrons.

It is highly desirable to have a computational approach which accurately includes electron-electron correlations and spin degree of freedom, and which can handle inhomogeneous systems with on the order of  $10^2$ – $10^3$  electrons. One such approach which

is in principle valid for any interacting electron system is density functional theory (DFT) [26, 27, 28]. There have been some attempts to apply density functional theory to the FQHE. Ferconi and Vignale [29] applied current density functional theory [30] to small, parabolically confined quantum Hall systems and showed that the current density functional theory gave good results for the ground state energy and spin polarization near  $\nu = 1$ . However, the energy gaps due to correlation effects were not included in that calculation. Ferconi, Geller and Vignale [31] also recently studied spin-polarized FQHE systems within the spirit of the DFT using an extended Thomas-Fermi approximation at low, but non-zero, temperatures. In this, the kinetic energy was treated as a local functional, as in the standard Thomas-Fermi approximation, while the exchange-correlation energy was included in a local density approximation (LDA). This extended Thomas-Fermi approximation is valid in the limit of very slowly varying confining potential. Ferconi, Geller and Vignale focused on the incompressible and compressible strips at an edge of an FQHE system, and obtained results in agreement with the predictions by Chklovskii, Shklovskii, and Glazman [24].

We have developed for the fractional quantum Hall effect an ensemble DFT scheme within the local density approximation, and have applied it to circularly symmetric quantum dots [32, 33]. In our approach, the kinetic energy is treated exactly, and the density represented by Kohn-Sham orbitals. The results are in good agreement with results obtained by semiclassical [23, 24, 31], Hartree-Fock [21, 22] (for cases where the correlations do not play a major role), and exact diagonalization methods [25]. Our calculations for spin-polarized systems show that the exchange and correlation effects of the FQHE are very well represented by the LDA and that our approach provides a computational scheme to model large inhomogeneous FQHE systems. We note that there exist previous formal DFTs for strongly correlated systems, in particular for high-temperature superconductors [34], and DFT calculations of high- $T_c$  materials [35] and transition-metal oxides [36]. However, ours are, to the best of our knowledge, the first practical LDA-DFT calculations of a strongly correlated system in strong magnetic fields, and demonstrate the usefulness of the LDA-DFT in studying large inhomogeneous FQHE systems. Recently, we have generalized our DFT approach to include spin degrees of freedom in an approximation in which the spin-quantization axis is parallel to the external magnetic field. While such an approximation cannot capture skyrmion-like excitations, in which the spin quantization axis is tumbling in space, it does demonstrate the existence of spin structures near edges of inhomogeneous systems consistent with numerical diagonalizations [25] and Hartree-Fock calculations [15]. We are presently working on extending the DFT approach to allow for the possibility of a tumbling spin quantization axis.

## Ensemble density functional theory approach for spin-polarized systems

In typical DFT calculations of systems of  $N_{el}$  electrons, the standard Kohn-Sham (KS) scheme [37] is implemented, in which the particle density  $n(\mathbf{r})$  is expressed in terms of a Slater determinant of  $N_{el}$  KS orbitals,  $\psi_i(\mathbf{r})$ . These obey an effective single-particle Schrödinger equation  $H_{eff} \psi_i = \epsilon_i \psi_i$ , which is solved self-consistently by occupying the  $N_{el}$  KS orbitals with the lowest eigenvalues  $\epsilon_i$ , and iterating. This scheme works well in practice for pure-state v-representable systems, for which the true electron density can be represented by a single Slater determinant of single-particle wavefunctions. However, when the KS orbitals are degenerate at the Fermi energy (which we identify with the largest  $\epsilon_i$  of the occupied orbitals) there is an ambiguity in how to occupy these degenerate orbitals. There exists an extension of DFT which is

formally able to deal with this situation. This extension is called ensemble DFT [27, 28], and in it, the density of the system is represented by an ensemble of Slater determinants of KS orbitals. However, while it can be shown using ensemble DFT that such a representation of the density is rigorous, it cannot be shown how the degenerate KS orbitals at the Fermi energy should be occupied, i.e., there has not been available a practical computational scheme for ensemble density functional theory.

We begin by first demonstrating that fractional quantum Hall systems are not in general pure-state  $v$ -representable, which means their densities cannot be obtained by a single Slater determinant of Kohn-Sham orbitals. Hence, an ensemble representation has to be used. Consider a uniform fractional quantum Hall system at filling factor  $\nu = 1/3$ . This density can be obtained by forming a density matrix of the form

$$\hat{D} = \frac{1}{3} \sum_{i=1}^3 |j_i\rangle \langle j_i| \quad (2)$$

Here,  $|j_i\rangle$  are the three possible degenerate Slater determinants obtained by filling every third single-particle orbital in the lowest Landau level. Using momentum eigenfunctions, we can write in occupation-number representation  $|j_1\rangle = |f100100100\rangle$ ,  $|j_2\rangle = |f010010010\rangle$ , and  $|j_3\rangle = |f001001001\rangle$ . The corresponding ensemble density is then

$$n_D(\mathbf{r}) = \text{Tr} \hat{D} \hat{n}(\mathbf{r}) = \frac{1}{3} \sum_{i=1}^3 n_i(\mathbf{r}) = \frac{1}{3} \frac{1}{2} \frac{q}{B}; \quad (3)$$

that is, the filling factor is fixed at  $\nu = 1/3$ . Because we can construct the correct ground state density from a density matrix of the form Eq. (2) with  $q > 2$ , it follows from a theorem by Levy [38] and Lieb [39] that this system then has a density which cannot be derived from a single ground state Kohn-Sham determinant, i.e.,  $n_D(\mathbf{r})$  is not pure-state  $v$ -representable. (This is true whenever we can write the ground state density of a system in the form of Eq. (2) with more than two terms.) However,  $n_D(\mathbf{r})$  is still associated with an external potential, and is ensemble representable.

Although ensemble DFT has been developed formally, there are in practice few examples of applications and calculations using ensemble DFT for ground state calculations. A significant aspect of our work is that we have developed an ensemble scheme which is practical and useful for the study of the FQHE. In ensemble DFT, any physical density  $n(\mathbf{r})$  can be represented by  $n(\mathbf{r}) = \sum_{m,n} f_{m,n} |j_{m,n}(\mathbf{r})|^2$ ; where  $f_{m,n}$  are occupation numbers satisfying  $0 \leq f_{m,n} \leq 1$ , and the orbitals  $|j_{m,n}\rangle$  satisfy the equation

$$\left( \frac{1}{2m} p^2 + \frac{e}{c} A(\mathbf{r})^2 + V_{\text{ext}}(\mathbf{r}) + V_H(\mathbf{r}) + V_{xc}(\mathbf{r}; B) \right) |j_{m,n}(\mathbf{r})\rangle = \epsilon_{m,n} |j_{m,n}(\mathbf{r})\rangle; \quad (4)$$

where  $r^2 A(\mathbf{r}) = B(\mathbf{r})$ . In equation (4),  $V_H(\mathbf{r})$  is the Hartree interaction of the 2D electrons, and, as usual,  $V_{xc}(\mathbf{r}; B)$  is the exchange-correlation potential, defined as a functional derivative of the exchange-correlation energy  $E_{xc}[n(\mathbf{r}); B]$  of the system with respect to density:  $V_{xc}(\mathbf{r}; B) = \frac{E_{xc}[n(\mathbf{r}); B]}{n(\mathbf{r})}$ . (We will hereafter not explicitly indicate the parametric dependence of  $V_{xc}$  and  $E_{xc}$  on  $B$ .) For the case of the FQHE, we know that the exchange-correlation potential will be crucial, as it contains all the effects of the electron correlations which cause the FQHE in the first place, and a major part of the DFT application is to come up with an accurate model of  $E_{xc}$  and so of  $V_{xc}$ . Leaving this question aside for a moment, and assuming that we have succeeded in doing so, the practical question is then how to determine the KS orbitals and their occupancies in the presence of degeneracies. We have devised an empirical scheme, which produces a set of occupancies for the KS orbitals which satisfy some minimum requirements, namely

(a) the scheme converges to physical densities (to the best of our knowledge) for FQHE systems, (b) it reproduces finite temperature DFT distributions at finite temperatures, and (c) it reproduces the standard Kohn-Sham scheme for systems whose densities can be represented by a single Slater determinant.

In our scheme, we start with input occupancies and single-particle orbitals and iterate the system  $N_{eq}$  times using the KS scheme. The number  $N_{eq}$  is chosen large enough (about 20-40 in practical calculations) that the density is close to the final density after  $N_{eq}$  iterations. If the density of the system could be represented by a single Slater determinant of the KS orbitals, we would now essentially be done. However, in this system there are now in general many degenerate or near-degenerate orbitals at the Fermi energy. After each iteration, the Kohn-Sham scheme chooses to occupy the  $N_{el}$  orbitals with the lowest eigenvalues, corresponding to making a distinct Slater determinant of these orbitals. But there will be small fluctuations in the density between each iteration, which cause a different subset of these (near) degenerate orbitals to be occupied after each iteration. This corresponds to constructing different Slater determinants after each iteration, and the occupation numbers  $f_{m,n}$  of these orbitals are zero or unity more or less at random after each iteration. This means that the computations will never converge. However, the average occupancies, i.e., the occupancies averaged over many iterations, become well defined and approach a definite value, e.g.,  $1/3$  for orbitals localized in a region where the local filling factor is close to  $\nu = 1/3$ . Therefore, we use these average occupancies to construct an ensemble by accumulating running average occupancies  $\langle f_{m,n} \rangle$  after the initial  $N_{eq}$  iterations

$$\langle f_{m,n} \rangle = \frac{1}{(N_{it} - N_{eq})} \sum_{i=N_{eq}+1}^{N_{it}} f_{m,n,i}; \quad (5)$$

where  $f_{m,n,i}$  is the occupation number (0 or 1) of orbital  $m,n$  after the  $i$ th iteration, and use these to calculate densities. Thus, our algorithm essentially picks a different (near) degenerate Slater determinant after each iteration, and these determinants are all weighted equally in the ensemble. It is clear that this scheme reduces to the KS scheme for which the density can be represented by a single Slater determinant of KS orbitals (for which the KS scheme picks only the one Slater determinant which gives the ground state density) for  $N_{eq}$  large enough. Moreover, we have numerically verified that a finite-temperature version of our scheme converges to a thermal ensemble at finite temperatures down to temperatures of the order of  $10^{-3} \hbar \omega_c / k_B$ . We have also performed some Monte Carlo simulations about the ensemble obtained by our scheme. In these simulations, we used a Metropolis algorithm to randomly change the occupation numbers about our converged solution, keeping the chemical potential fixed. The free energy of the new set of occupation numbers was calculated self-consistently. If the free energy decreased, this set was kept, and if the free energy increased, the set was kept if a random number was smaller than  $\exp[-\Delta F / k_B T]$ , where  $\Delta F$  is the change in free energy, and  $T$  a fictitious temperature. The results were that to within numerical accuracy our ensemble DFT scheme gives the lowest free energy. As a condition for convergence, we typically demanded that the difference between the input and output ensemble densities,  $n_{in}(r)$  and  $n_{out}(r)$ , of one iteration should satisfy

$$\frac{1}{N_{el}} \sum_{i=0}^Z |n_{in}(r) - n_{out}(r)| dr < 5 \cdot 10^{-4}; \quad (6)$$

Practical density functional theory calculations hinge on the availability of good approximations for the exchange-correlation potential  $V_{xc}$ , which enters in the effective

Schrodinger equation for the KS orbitals. The simplest, and probably the most commonly used, approximation is the local density approximation (LDA). In this approximation, the exchange-correlation energy is assumed to be a local function of density, so that the total exchange-correlation energy consists of contributions from the local density of the system. Thus, in this approximation one writes  $E_{xc} = N \int d\mathbf{r} \epsilon_{xc}(\mathbf{r}) n(\mathbf{r})$ ; where  $\epsilon_{xc}(\mathbf{r})$  is the exchange-correlation energy per particle in a homogeneous system of constant density  $n = \frac{1}{(2\pi)^3} \int d\mathbf{k}$  and  $\epsilon_{xc}$  is the exchange-correlation energy per particle in a homogeneous system of constant density  $n = \frac{1}{(2\pi)^3} \int d\mathbf{k}$  and  $\epsilon_{xc}$  is the exchange-correlation energy per particle in a homogeneous system of constant density  $n = \frac{1}{(2\pi)^3} \int d\mathbf{k}$ . In other words, in the LDA one assumes that the system is locally homogeneous, i.e., the system can locally be approximated to have the energy per particle of an infinite, homogeneous system of the local density. This approximation obviously makes sense if the density of the system varies on a very long length scale, while it could be questionable for systems in which the density varies on some microscopic length scale. However, experience has shown that the LDA often works surprisingly well, even for systems in which the electron density is strongly inhomogeneous [26]. In the FQHE, the length scale of exchange-correlation interactions and density fluctuations is given by the magnetic length  $\lambda_B$  due to the Gaussian falloff of any single-particle basis in which the interacting Hamiltonian is expanded. The densities are relatively smooth on this length scale, which gives us additional hope that the LDA will work well for the FQHE, too. In addition, the cusps in the exchange-correlation energy will suppress density fluctuations, so in this sense one can actually expect the basic physics of the FQHE to make the LDA a good approximation.

We construct our exchange-correlation energy by writing

$$\epsilon_{xc}(\mathbf{r}) = \epsilon_{xc}^{LM}(\mathbf{r}) + \epsilon_{xc}^C(\mathbf{r}) \quad (7)$$

Here,  $\epsilon_{xc}^{LM}(\mathbf{r})$  is a smooth interpolation formula (due to Levesque, Weiss and MacDonald [40]) between ground state energies at some rational fillings. The second term,  $\epsilon_{xc}^C(\mathbf{r})$ , is all-important for the study of the FQHE. This term contains the cusps in the ground state energy which cause the FQHE. Here we have used a simple model which captures the essential physics. We model  $\epsilon_{xc}^C(\mathbf{r})$  by constructing it to be zero at values of  $\nu = p/q$  which display the FQHE. Near  $\nu = p/q$ ,  $\epsilon_{xc}^C(\mathbf{r})$  is linear and has at  $\nu = p/q$  a discontinuity in the slope related to the chemical potential gap  $\Delta = q(j_p + j_h)$ . Here  $j_{p,h}$  are the quasiparticle (hole) creation energies which can be obtained from the literature [41, 42] at fractions  $\nu = p/q$ . Farther away from  $\nu = p/q$ ,  $\epsilon_{xc}^C(\mathbf{r})$  decays to zero. Finally, in the LDA  $V_{xc}(\mathbf{r})$  is obtained from  $\epsilon_{xc}(\mathbf{r})$  as  $V_{xc}(\mathbf{r}) = \frac{\partial \epsilon_{xc}(\mathbf{r})}{\partial n(\mathbf{r})}$  at constant  $B$ . In our calculations, we restrict ourselves to include only the cusps at  $\nu = 1/3, 2/5, 3/5$  and  $\nu = 2/3$  (and the analogous ones at  $4/3, 7/5, 8/5$  and  $5/3$ ), which are the strongest fractions. These are some of the fractions of the form  $\nu = \frac{p}{(2p-1)}$  generated by the so-called  $V_1$ -model, in which only the pseudo-potential  $V_1$  is included.

A technical difficulty arises in the LDA: the discontinuities in  $V_{xc}(\mathbf{r})$  in the LDA give rise to a numerical instability. The reason is that an arbitrarily small fluctuation in charge density close to an FQHE fraction gives rise to a finite change in energy. Imagine that the local filling factor  $\nu(\mathbf{r})$  in some neighborhood of a point  $\mathbf{r}$  is very close to, but less than, say,  $1/3$  after one iteration. In this neighborhood, the local exchange-correlation potential will then form a potential well with sharp barriers at the points around  $\mathbf{r}$  where  $\nu(\mathbf{r}) = 1/3$ . During the next iteration, charge will then be poured into this well. As a result, the local filling factor will after this iteration exceed  $1/3$ , and in this neighborhood  $V_{xc}$  now forms a potential barrier of finite height. So in the next iteration, charge is removed from this neighborhood, and so on. We can see that this leads to serious convergence problems. To overcome this, we made the compressibility of the system finite, but very small, corresponding to a finite, but very



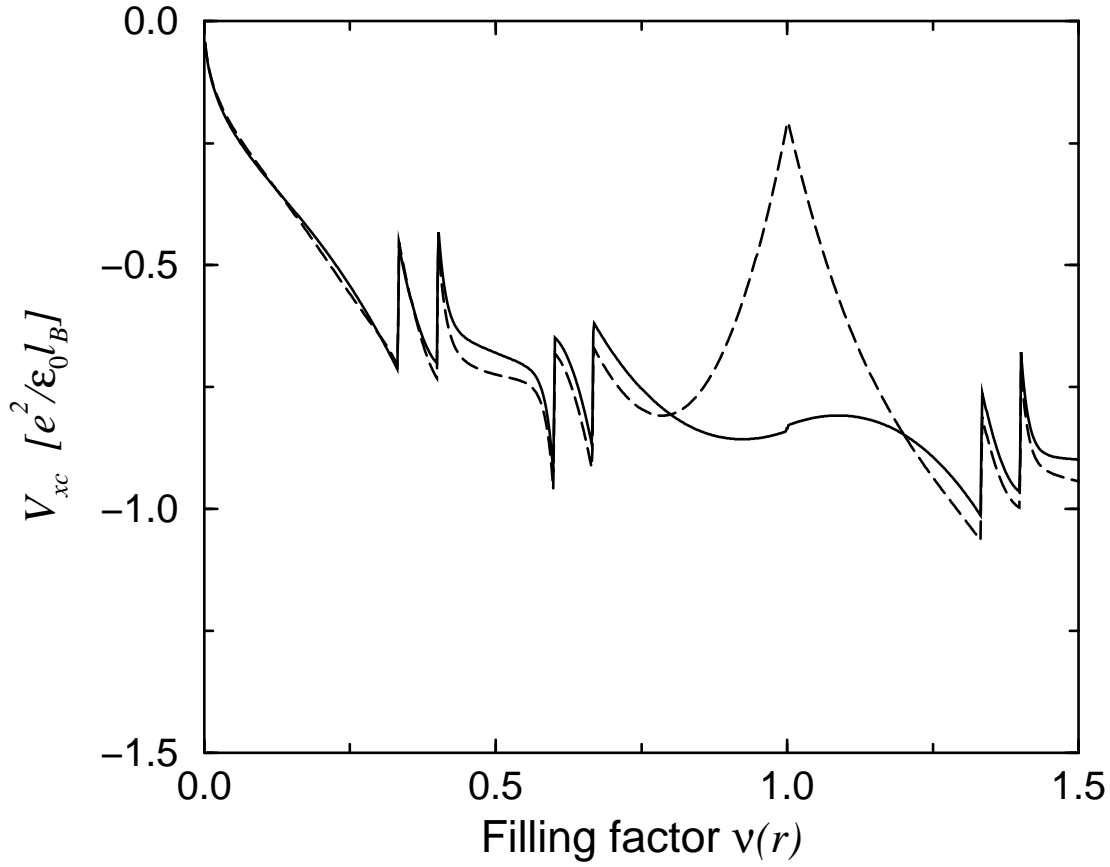


Figure 2. Exchange-correlation potentials  $V_{xc}^*$  (solid line) and  $V_{xc}^\#$  (dashed line) for a spin-polarized system as function of filling factor in units of  $e^2/(\epsilon_0 l_B)$  for 0  $\leq \nu(r) \leq 1.5$ . The increase in  $V_{xc}$  at an FQHE filling factor occurs over a range of filling factor of 0.002.

large, curvature instead of a point-like cusp in  $\mu_{xc}$  at the FQHE fractions. In other words, instead of having a step-like discontinuity in the chemical potential, it rises smoothly an amount over an interval in the filling factor. What we found worked very well in practice was to have the discontinuity in chemical potential occur over an interval of filling factor of magnitude  $10^{-3}$ . This corresponds to a sound velocity of about  $10^6$  m/s in the electron gas, which is three orders of magnitude larger than the Fermi velocity of a 2D electron gas at densities typical for the FQHE. In general, the finite compressibility does not lead to any spurious physical effects so long as the energy of density fluctuations on a size of the order of the system's size is larger than any other relevant energy in the problem. The only noticeable effect is that incompressible plateaus, at which the density would be perfectly constant were the compressibility zero, will have density fluctuations on a scale of  $\lambda_D$ . Figure 2 depicts  $V_{xc}$  for a spin-polarized system used in our calculations as a function of filling factor.

#### Applications to spin-polarized quantum dots

We have self-consistently solved the KS equations Eqs. (4) for a spin-polarized quantum dot in a parabolic external potential,  $V_{\text{ext}}(r) = \frac{1}{2}m\omega^2 r^2$ , by expanding the KS orbitals  $\psi_{mn}(r) = e^{im\phi} \phi'_{mn}(r)$  in the eigenstates of  $H_0 = \frac{1}{2m}p^2 + \frac{e}{c}A(r)^2$ . We

use the cylindrical gauge,  $A(r) = \frac{1}{2}Br^2$ , and include the four lowest Landau levels ( $n = 0, \dots, 3$ ). We chose the static dielectric constant  $\epsilon_0 = 12.4$ , appropriate for GaAs, and a confining potential of strength  $\beta\hbar = 1.6$  meV.

The use of our LDA-DFT scheme is illustrated by a study of the edge reconstruction of the quantum dot as a function of magnetic field strength. As is known from Hartree-Fock and exact diagonalizations [21, 22, 25, 18, 19], for strong confinement the quantum dot forms a maximum density droplet in which the density is uniform at  $\rho = 1$  in the interior, and falls off rapidly to zero at  $r = \sqrt{2N_{el}}/B = r_0$ . As the magnetic field strength increases, a "lump" of density breaks off, leaving a "hole" or deficit at about  $r = r_0$ . This effect is due to the short-ranged attractive exchange interaction: it is energetically favorable to have a lump of density break off so that the system can take advantage of the exchange energy in the lump. As  $B$  is further increased, the correlations will cause incompressible strips with densities  $\rho = p/q$  to appear [23, 24, 43, 31] on the edges, and incompressible droplets to form in the bulk at densities  $\rho = p/q$ . Figure 3 depicts various stages of edge reconstruction obtained by us as the magnetic field strength is increased. The value of  $B$  for which the exchange lump appears compares very well with the value found by De Chamion and Wen [22] in Hartree-Fock and numerical diagonalizations. At higher fields still, incompressible strips appear at the edges, and incompressible droplets are formed in the bulk.

Figure 4 depicts the eigenvalues of the KS orbitals for  $N_{el} = 40$ , and  $B = 4 \pm 0.1$  T. The dashed line indicates the chemical potential of the system. This figure then shows that all KS orbitals in the bulk are in fact degenerate. It may at first seem paradoxical that the eigenvalues are degenerate on an incompressible strip, since, according to the picture by Chklovskii, Shklovskii, and Glazman [24], on such a strip the density is constant, while the total potential varies (since the electrons cannot screen the external potential). If the total potential varies, then ought not the the eigenvalues of the KS orbitals localized on that strip vary, too, since these then in general are subjected to different potential energies? The problem with this argument as applied to DFT is that it ignores the effect of the exchange-correlation potential. As the external and Hartree potentials vary across the strip, the exchange-correlation potential varies across its discontinuity so as to completely screen out the external and Hartree potentials. The discontinuity in  $V_{xc}$  does not mean that this potential is fixed at the lower limit of its discontinuity while the density is fixed at an incompressible strip. What it does mean, is that  $V_{xc}$  is free to achieve any value across its discontinuity so as to completely screen out the external and Hartree potentials. In this way, it is perhaps better to think of incompressibility as the limit of a finite compressibility approaching zero. A strip can then remain incompressible with constant density so long as  $V_{xc}$  can screen the external and Hartree potentials, so the width of the incompressible strip is given by the distance over which the external plus Hartree potentials varies an amount given by the energy gap associated with the density at that strip. Also, all bulk KS states are degenerate at the chemical potential. When a single particle is added, the chemical potential simply increases a small amount, and all KS orbitals are again degenerate at the chemical potential.

We have also tested the accuracy of our ensemble DFT-LDA approach by comparing our results for a six-electron system in a confining parabolic potential with the numerical diagonalization results by Yang, MacDonald and Johnson [25]. Figure 5 depicts angular momentum vs. magnetic field strength for this system. For better comparison with the numerical diagonalizations, we used here only basis states in the lowest Landau level ( $n = 0$ ). There are clear plateau structures in the angular momenta, and readily identifiable transitions, such as the initial instability of the maximum density

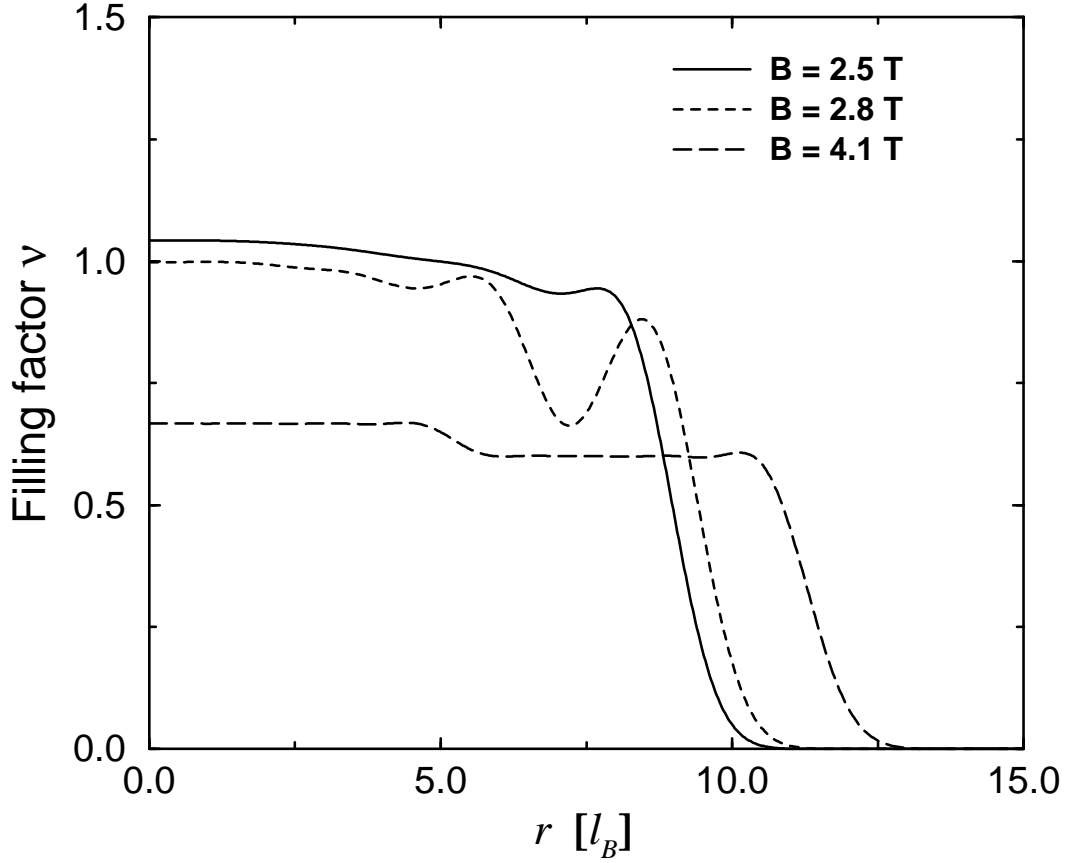


Figure 3. Edge reconstruction of a quantum dot as the magnetic field strength is increased. Plotted here is the local filling factor  $\nu(r)$  for a parabolic quantum dot with  $\hbar\omega_c = 1.6$  meV and 40 electrons. For magnetic field strengths  $B < 2.5$  T the dot forms a maximum density droplet, and for  $B \geq 2.8$  T, an exchange hole is formed. For stronger magnetic fields, incompressible regions form, separated by compressible strips.

droplet at about 2.8 T, and a formation of a  $\nu = 1/3$  droplet at about 5.3 T. The agreement is in general very good, in particular considering that (a) the DFT calculations are not constructed to give quantized angular momentum, (b) there are no adjustable parameters in our approach, and (c) the numerical diagonalizations used the full Coulomb interaction, while our DFT approach only included the cusps at  $\nu = 1/3; 2/5; 3/5$ , and  $\nu = 2/3$ . The Levesque-Weiss-MacDonald interpolation formula used here tends to overestimate the magnitude of the exchange-correlation potential around  $\nu = 1/2$ , which increases the values at which transitions occur. For example, the  $\nu = 1/3$  droplet formation occurs at 5.29 T in the numerical diagonalization, but at about 5.5 T in the DFT-LDA calculation. The overestimation of the exchange-correlation potential also leads to decreased angular momenta at the different plateaus. For example, while the  $\nu = 1/3$  droplet has angular momentum 45 in the numerical diagonalization, examination of the density profiles shows that the formation of a  $\nu = 1/3$  droplet occurs at an angular momentum of about 40 in our calculations. We are presently working on improving the exchange-correlation energy for better agreement with numerical diagonalization. Initial calculations give highly accurate results for the maximum density droplet instability, and the formation of a  $\nu = 1/3$  droplet.

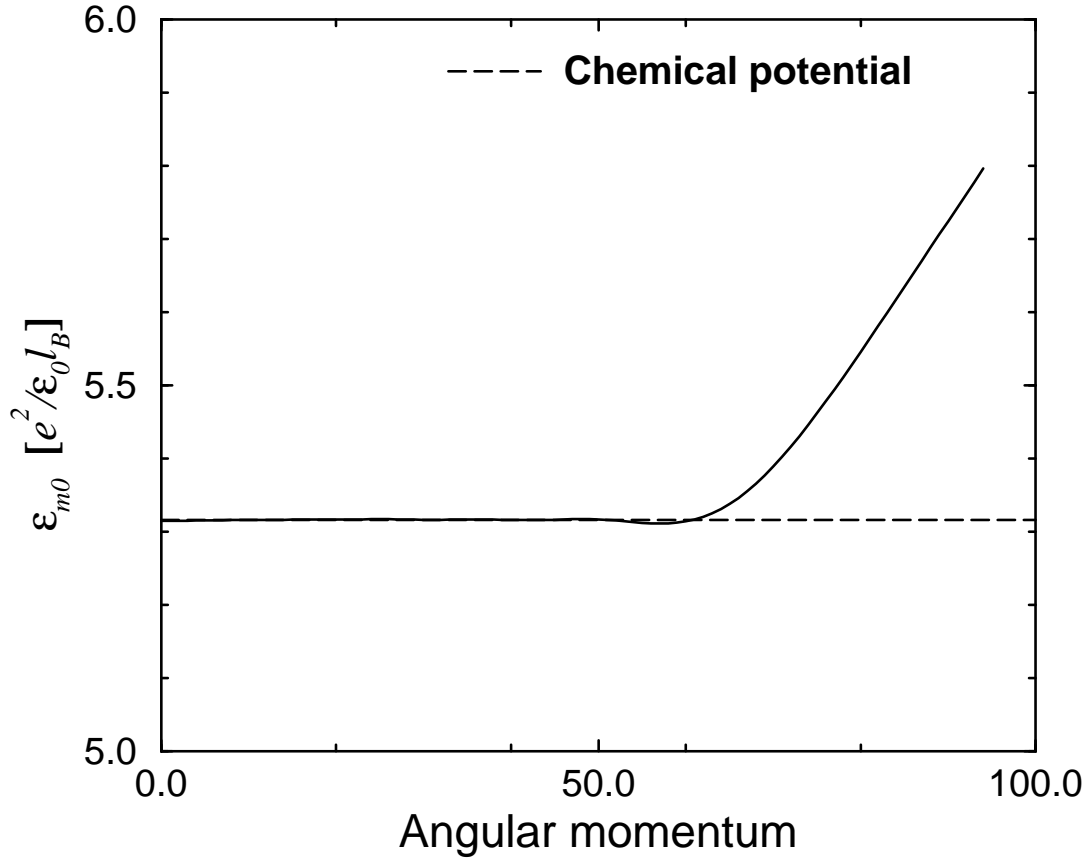


Figure 4. Eigenvalues of the lowest Landau level Kohn-Sham orbitals for  $N_{el} = 40$  and  $B = 4.10$  T as a function of angular momentum quantum number. The chemical potential is indicated by the dashed line.

Including spin degrees of freedom

As mentioned above, due to the small effective Lande  $g$ -factor in GaAs, the spin degree of freedom play an important role in quantum Hall systems, in spite of the large applied magnetic fields. We have begun to generalize our ensemble density functional approach to include the spin degree of freedom. In general [44], spin density functional theory has to be based on the single-particle density matrix  $\rho_{\sigma}(\mathbf{r}) = \langle \hat{\psi}_{\sigma}^{\dagger}(\mathbf{r}) \hat{\psi}_{\sigma}(\mathbf{r}) \rangle$ , where  $\hat{\psi}_{\sigma}(\mathbf{r})$  is the annihilation operator for an electron of spin  $\sigma$  at position  $\mathbf{r}$ . However, in the presence of a uniform external magnetic field  $\mathbf{B} = B \hat{z}$ , the  $z$ -component of total electron spin,  $\hat{S}_z$ , commutes with the Hamiltonian, and it is a reasonable approximation to take  $\rho_{\sigma}(\mathbf{r})$  to be diagonal in the spin indices,  $\rho_{\sigma}(\mathbf{r}) = n_{\sigma}(\mathbf{r}) \delta_{\sigma\sigma}$ , with  $n_{\sigma}(\mathbf{r})$  the up- and down-spin densities. (Note, however, that this restriction has to be lifted in order to study skyrmion-like spin textures, which complicates the formalism a great deal.) We now obtain two sets of KS equations, one for each spin direction:

$$\left( -\frac{\hbar^2}{2m} \nabla^2 + \frac{e}{c} \mathbf{A}(\mathbf{r}) \cdot \nabla + V_{\text{ext}}(\mathbf{r}) + V_H(\mathbf{r}) + V_{xc}(\mathbf{r}; B) + g_0 B \right) \psi_{m,n}(\mathbf{r}) = \epsilon_{m,n} \psi_{m,n}(\mathbf{r}) \quad (8)$$

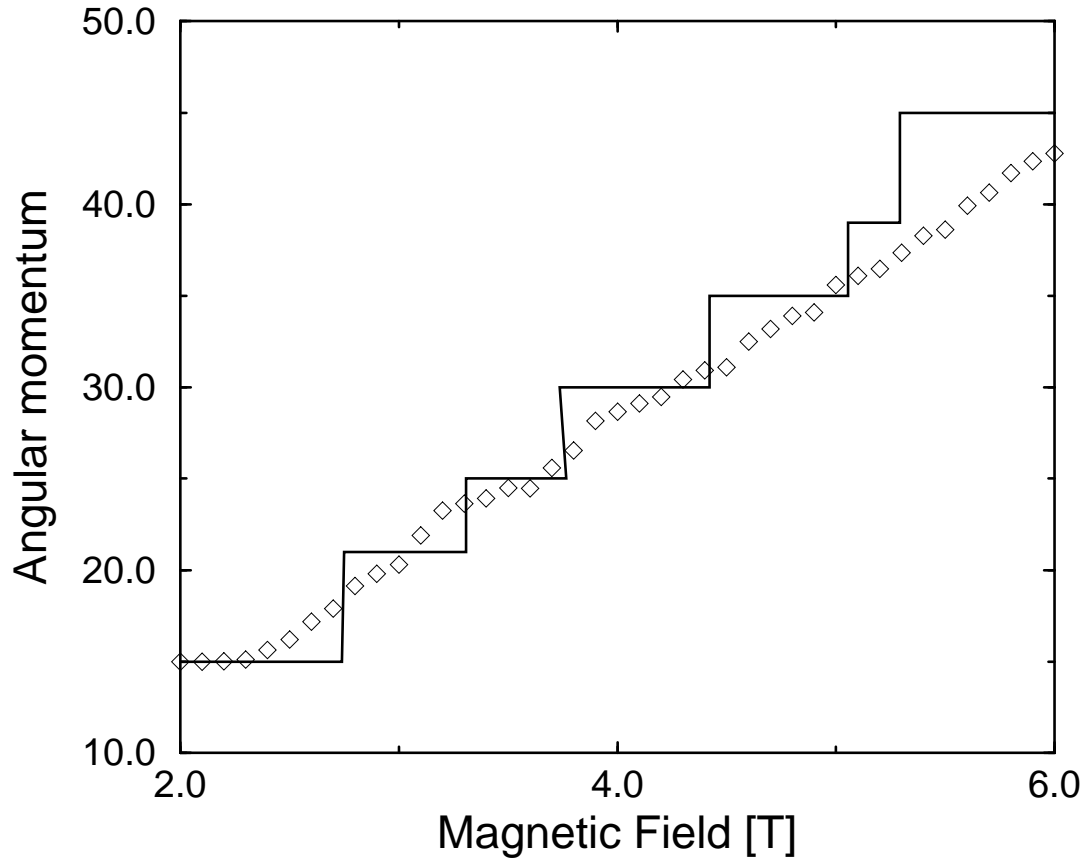


Figure 5. Angular momentum vs. magnetic field strength for a six-electron droplet in a parabolic potential with  $\hbar = 2.0$  meV. The solid line is from numerical diagonalizations (Ref. 25), and the diamonds are from our DFT-LDA calculations.

Here,  $\hbar = 1$ ,  $\hbar_0$  is the Bohr magneton, and in the local spin density approximation (LSDA) the exchange-correlation potentials are

$$V_{xc,i}(\mathbf{r}; \mathbf{B}) = \frac{\partial}{\partial n} [n_{xc}(n_\uparrow; n_\downarrow; \mathbf{B})] :_{n=n(\mathbf{r})} \quad (9)$$

It is more convenient to work with filling factor  $\nu(\mathbf{r}) = 2 \frac{e}{B} n(\mathbf{r})$  and spin polarization  $\nu_\pm = (n_\pm - n_\mp) / (n_\pm + n_\mp)$ , in terms of which we have

$$\begin{aligned} V_{xc,\uparrow} &= \frac{\partial}{\partial \nu} (\epsilon_{xc}) + (1 - \nu_\pm) \frac{\partial}{\partial \nu_\pm} \epsilon_{xc}; \\ V_{xc,\downarrow} &= \frac{\partial}{\partial \nu} (\epsilon_{xc}) - (1 + \nu_\pm) \frac{\partial}{\partial \nu_\pm} \epsilon_{xc}; \end{aligned} \quad (10)$$

where now the exchange-correlation energy per particle in a homogeneous system with a filling factor  $\nu$  and polarization  $\nu_\pm$  has to be approximated. Except for a few data points obtained by small system numerical diagonalizations[45], this is largely unknown. In order to obtain a useful approximation, we start by considering only the exchange energy  $E_x[\uparrow; \downarrow]$ . Since the exchange interaction only couples electrons with parallel spins, we have

$$E_x[\uparrow; \downarrow] = \frac{1}{2} E_x[\uparrow; \uparrow] + \frac{1}{2} E_x[\downarrow; \downarrow]; \quad (11)$$

In two dimensions, the exchange energy scales as  $n^{3/2}$ , so using Eq. (11), we can correctly interpolate between a fully polarized system ( $s = 1$ ) and a completely unpolarized one ( $s = 0$ ) by writing

$$x[s; \eta] = x[s; \eta = 1] + [x[s; \eta = 0] - x[s; \eta = 1]]f(\eta); \quad (12)$$

where

$$f(\eta) = \frac{(1 + \eta)^{3/2} + (1 - \eta)^{3/2}}{2} - \frac{2^{3/2}}{2}: \quad (13)$$

We then use the same interpolation for the correlation energy (excluding the cusps for a moment), as was first done by von Barth and Hedin [44] for the three-dimensional electron gas in zero magnetic field, and write

$$\begin{aligned} E_{xc}^0[s; \eta] &= E_{xc}^{LW M}[s; \eta = 1] + [E_{xc}^0[s; \eta = 0] - E_{xc}^0[s; \eta = 1]]f(\eta) \\ E_{xc}^{LW M}[s; \eta = 1] &+ E_{xc}^0[s; \eta]f(\eta): \end{aligned} \quad (14)$$

The function  $E_{xc}^0[s; \eta]$  can be obtained by calculating the energy difference between polarized and unpolarized systems using data obtained from small system numerical diagonalizations [45]. A accurate value for the exchange-correlation energy for  $s = 0$  and  $s = 1$  is not available, but it is a useful approximation to assume that the different spin directions are completely uncorrelated at  $s = 0$  and  $s = 1$ , which gives  $E_{xc}^0[s = 1; \eta = 0] = E_{xc}^0[s = 1; \eta = 2; \eta = 0]$ . This approximation also gives a good value for the exchange enhancement, which is the energy required to flip a spin in a polarized system at  $s = 1$ .

So far, we have constructed a function  $E_{xc}^0[s; \eta]$  which gives a smooth interpolation for the exchange-correlation energy for any value of  $s$  and  $\eta$ . What is left is to add the cusps to this function. We already have a good approximation for this at  $s = 1$ . We now need to extend this approximation to arbitrary values of  $s$ . Very little is known about the cusps, i.e., the energy gaps, for arbitrary polarizations. It is known that there is a gap for unpolarized systems at fillings  $\nu = 2/5$ ,  $\nu = 3/5$ , and  $\nu = 2/3$ . The gap, and thus the cusps, occur at very special 'magic' configurations at which the system can take advantage of a particularly low correlation energy. Therefore, it seems plausible that for a given value of  $s$ , say  $s = 2/5$ , there cannot be an energy gap for any value of  $\eta$  between 0 and 1. In order to incorporate this assumption into a usable approximation, we interpolate our cusp energy constructed for polarized systems,  $E_{xc}^C[s; \eta]$ , to arbitrary polarizations by multiplying it by a function  $g(\eta)$  which is unity at  $\eta = 0$  and  $\eta = 1$ , and vanishes away from these values of polarization. All together, then, we have

$$E_{xc}[s; \eta] = E_{xc}^{LW M}[s; \eta] + E_{xc}^0[s; \eta]f(\eta) + E_{xc}^C[s; \eta]g(\eta): \quad (15)$$

Figure 2 depicts  $V_{xc}$  (here for  $s = 1$ ) used in our calculations.

We have applied this spin ensemble DFT to study the phase diagram of a maximum density droplet. For large values of the Lande-factor  $g$ , the maximum density droplet is fully polarized, and as the magnetic field is increased, there is an instability to forming a spin-polarized exchange-hole. But for small values of  $g$ , the instability is towards forming a spin structure at the edge. The value of  $g$  separating the spin-polarized and spin-structured instabilities,  $g_c = g_B B = (e^2 / \epsilon_0 \hbar^2) \approx 0.05$ , is in good agreement with the value found for  $g_c \approx 0.03$  found from numerical diagonalizations of parabolic dots by Yang, MacDonald and Johnson [25], and consistent with the value obtained in calculations by Kivelson et al. [15], who used a Hartree-Fock approximation in which the spin axis was allowed to tumble. They obtained a value  $g_c = 0.17$  for an infinite Hallbar.

In conclusion, we have showed that ensemble density functional theory can be applied to the FQHE. This opens the door to doing realistic calculations for large systems. We believe that our results are also significant in that they are the first LDA-DFT calculations of a strongly correlated system in a strong magnetic field, and they are (to the best of our knowledge) the first practical ensemble DFT calculations. We find excellent agreement between our ensemble DFT calculations and numerical diagonalizations and Hartree-Fock calculations. Preliminary calculations including spin degrees of freedom are consistent with numerical diagonalizations and Hartree-Fock calculations. We are presently working on improving the exchange-correlation energy as a function of density and polarization. Finally, the spin DFT presented here cannot be used to study skyrmion-like structures, in which the spin density vector is tumbling in space. Work is presently underway, together with J. Kinnaret (Chalmers University of Technology) to develop such a theory.

The authors would like to thank M. Ferconi, M. Geller and G. Vignale for helpful discussions and for sharing their results prior to publications, K. Burke and E. K. U. Gross for useful comments about the DFT, and M. Levy for a discussion about ref. [38]. O. H. would like to thank Chalmers Institute of Technology, where part of the numerical work was done. This work was supported by the NSF through grants DMR 93-01433 and DMR 96-32141.

## REFERENCES

1. The quantum Hall effect, edited R.E. Prange and S.M. Girvin (Springer, New York 1987).
2. K. von Klitzing, G. Dorda, and M. Pepper, Phys. Rev. Lett. 45, 494 (1980).
3. D.C. Tsui, H.L. Stormer, and A.C. Gossard, Phys. Rev. Lett. 48, 1559 (1982).
4. R.B. Laughlin, Phys. Rev. Lett. 50, 1395 (1983).
5. F.D.M. Haldane, Phys. Rev. Lett. 51, 605 (1983).
6. B.I. Halperin, Phys. Rev. B 25, 2185 (1982).
7. See, for example, A.H. MacDonald, in Quantum Transport in Semiconductor Microstructures, edited by B. Kramer (Kluwer Academic, 1996).
8. P.L. McEuen, E.B. Foxman, Jari Kinnaret, U. Meirav, M.A. Kastner, Ned S. Wingreen, and S.J. Wind, Phys. Rev. B 45, 11 419 (1992).
9. O. Klein, C. de C. Cham on, D. Tang, D.M. Abusch-Magder, U. Meirav, X.-G. Wen, M.A. Kastner, and S.J. Wind, Phys. Rev. Lett. 74, 785 (1995).
10. N.B. Zhitenev, M. Brodsky, R.C. Ashoori, M.R. Melloch, SISSA report cond-mat/9601157.
11. N.B. Zhitenev, R.J. Haug, K. von Klitzing, and K. Eberl, Phys. Rev. Lett. 71, 2292 (1993); G. Ernst, N.B. Zhitenev, R.J. Haug, K. von Klitzing, and K. Eberl, Surf. Sci. 361/362, 102 (1996).
12. J.M. Shilton et al., J. Phys. Condens. Mat. 8, L337 (1996); A. Knabchen and Y.B. Levinson, SISSA report cond-mat/9608074.
13. S.L. Sondhi, A. Karlhede, S.A. Kivelson and E.H. Rezayi, Phys. Rev. B 47, 16 419 (1993).
14. S.E. Barrett, D. Dabbagh, L.N. Pfeiffer and K.W. West, Phys. Rev. Lett. 74, 5112 (1995).
15. A. Karlhede, S.A. Kivelson, K. Lejnell and S.L. Sondhi, SISSA report cond-mat/9605095.
16. X.-G. Wen, Phys. Rev. B 44 5708 (1991).
17. J.K. Jain and T. Kawamura, Europhys. Lett. 29, 321 (1995).
18. L. Breys, Phys. Rev. B 50, 11 861 (1994).
19. D.B. Chklovskii, Phys. Rev. B 51, 9895 (1995).
20. Eyal Goldman and Scott R. Renn PRB 1996?
21. A.H. MacDonald, S.R.E. Yang and M.D. Johnson. Aust. J. Phys. 46, 345 (1993).
22. C. de C. Cham on and X.G. Wen, Phys. Rev. B 49, 8227 (1994).
23. C.W.J. Beenakker, Phys. Rev. Lett. 64, 216 (1990).
24. D.B. Chklovskii, B.I. Shklovskii, and L.I. Glazman, Phys. Rev. B 46, 4026 (1992).
25. See, for example, S.-R. Eric Yang, A.H. MacDonald, and M.D. Johnson, Phys. Rev. Lett. 71, 3194 (1993).

26. W .Kohn and P.Vashista in Theory of the Inhomogeneous Electron Gas, edited by S.Lundqvist and N.March (Plenum , New York, 1983).
27. Density Functional Theory: an Approach to the Quantum Many-Body Problem , by R.M.Dreizler and E.K.U.Gross (Springer, Berlin 1990).
28. Density-Functional Theory of Atoms and Molecules, by R.G.Parr and W .Yang (Oxford University Press, New York, 1989).
29. M .Ferconi and G .Vignale, Phys. Rev. B 50, 14 722 (1994).
30. G .Vignale and M .Rasolt, Phys. Rev. Lett. 59, 2360 (1987); Phys. Rev. B 37, 10 685 (1988).
31. M .Ferconi, M .Geller and G .Vignale, Phys. Rev. B 52, 16 357 (1995).
32. O .Heinonen, M .I.Lubin, and M .D .Johnson, Phys. Rev. Lett. 75, 4110 (1995).
33. O .Heinonen, M .I.Lubin and M .D .Johnson, Int. J. Quant. Chem .: Quant. Chem . Symposium 30, 231 (1996).
34. E.K.U.Gross, L.N.de Oliveira and W .Kohn, Phys. Rev. A 37, 2805 (1988); Phys. Rev. A 37, 2809 (1988).
35. W .Pickett, Rev. Mod. Phys. 61, 433 (1989).
36. A .Svane and O .Gunnarsson, Phys. Rev. Lett. 65, 1148 (1990); Z.Szotek, W .Temmerman and H .Winter, Phys. Rev. B 47, 4029 (1993).
37. W .Kohn and L.J.Sham , Phys. Rev. 140, A1133 (1965).
38. M .Levy, Phys. Rev. A 26, 1200 (1982); M .Levy and J.P.Perdew in Density Functional Methods in Physics, edited by R.M.Dreizler and J.da Providencia (Plenum , New York 1985).
39. E.H.Lieb, Int. J. Quant. Chem . 24, 243 (1983).
40. D .Levesque, J.J.Weiss and A.H.MacDonald, Phys. Rev. B 30, 1056 (1984).
41. R.Morf and B.I.Halperin, Phys. Rev. B 33, 221 (1986).
42. N.d'Ambrosio and R.Morf, Phys. Rev. B 40, 6108 (1989).
43. B.Y.Gelfand and B.I.Halperin, Phys. Rev. B 49, 1994.
44. U.von Barth and L.Hedin, J. Phys. C 5, 1629 (1972).
45. For a comprehensive reference, see The Quantum Hall Effects, by T.Chakraborty and P.Pietiläinen (Springer Verlag, Berlin 1995).